Pharm Res (2011) 28:2896–2909
DOI 10.1007/s11095-011-0491-9

RESEARCH PAPER

An Acetate Prodrug of a Pyridinol-Based Vitamin E Analogue

Omar M. Khdour • Jun Lu • Sidney M. Hecht

Received: 12 February 2011 / Accepted: 24 May 2011 / Published online: 6 July 2011
© Springer Science+Business Media, LLC 2011

ABSTRACT

Purpose To investigate of an approach to stabilize a novel pyridinol based α–tocopherol analogue (**1**) as a prodrug by acetylation of its phenol moiety.

Methods Biochemical indicators of oxidative stress in mitochondria were utilized to gain insight into the cytoprotective mechanism(s) of compound **1** acetate. Oxygen free radical scavenging activity was measured using DCF probe in a cultured cell model system that had been placed under oxidative stress. Lipid peroxidation was examined both in a cell-free system and in oxidatively stressed cultured cells. The bioenergetic parameters of mitochondria were evaluated by measuring mitochondrial membrane potential ($\Delta\psi_m$) and the MPT.

Results The present results suggest strongly that the antioxidant efficacy of compound **1** can be improved by using it as a prodrug. The tested prodrug has shown to be activated as a function of time, presumably due to susceptibility to enzymatic hydrolysis, and exhibits an antioxidant effect in time-dependent manner, providing a compound that is more effective than α-tocopherol acetate with regard to all protective properties studied.

Conclusions An effective approach to stabilize compound **1** was realized by using its acetate as a prodrug.

KEY WORDS analogue · antioxidant · prodrug · pyridinol · reactive oxygen species (ROS) · stability · α-tocopherol acetate

ABBREVIATIONS

AAPH	2,2'-azobis-(2-amidinopropane) dihydrochloride
BSO	L-buthionine-(*S*, *R*)-sulfoximine
C_{11} BODIPY$^{581/591}$	4,4-difluoro-5-(4-phenyl-1,3-butadienyl)-4-bora-3a, 4a-diaza-s-indacene-3-propionic acid
Calcein AM	calcein acetoxymethyl
DCF	dichlorofluorescein
DCFH-DA	dichlorodihydrofluorescein diacetate
DEM	diethyl maleate
DLPC	1, 2-dilinoleoylphosphatidylcholine
DMSO	dimethylsulfoxide
EBS	Eagle's balanced salt
FBS	fetal bovine serum
FCCP	carbonyl cyanide *p*-trifluoromethoxyphenylhydrazone
FRDA	Friedreich's ataxia
GSH	glutathione
HSSB	Hanks' balanced salt solution buffer
MEM	Eagle's minimal essential medium
ROS	reactive oxygen species
SOPC	1-stearoyl-2-oleoyl-phosphatidylcholine
TMRM	tetramethylrhodamine methyl ester
α-TOH	α-tocopherol
βFGF	basic fibroblast growth factor

INTRODUCTION

Mitochondria are key organelles that participate in essential cellular functions including energy metabolism, calcium homeostasis and programmed cell death (1–3). The main source of reactive oxygen species (ROS) in most cell types is the mitochondria (4,5); ROS are normally detoxified by an

Electronic Supplementary Material The online version of this article (doi:10.1007/s11095-011-0491-9) contains supplementary material, which is available to authorized users.

O. M. Khdour • J. Lu • S. M. Hecht (✉)
Biodesign Institute & Department of Chemistry & Biochemistry
Arizona State University
1001 South McAllister Avenue
Tempe, Arizona 85287, USA
e-mail: sidhecht@asu.edu

intricate network of defense mechanisms, including antioxidant enzymes and glutathione in the mitochondria and cytosol (6–8). Oxidative stress is an early event associated with mitochondrial dysfunction, where the accumulation of reactive oxygen species (ROS), such as the hydroxyl radical, superoxide anion, and hydrogen peroxide, are believed to play a major role in the pathophysiology of degenerative and mitochondrial diseases (9–14). Oxidative stress describes a condition in which cellular antioxidant defenses are insufficient to keep the levels of ROS below a toxic threshold. The discovery that mitochondrial dysfunction underlies the pathogenesis of many neurodegenerative and mitochondrial diseases has led to new therapeutic strategies aimed at ameliorating and restoring mitochondrial function. Mitochondrial disease therapies have been envisioned using a variety of small molecule drugs (15–17).

There is growing interest in the development of antioxidants that have increased levels of stability, solubility and pharmacological activity. The antioxidant properties of α-tocopherol, a major biological radical quencher, are attributed to its phenolic structure (18,19). Tocopherols mediate their antioxidant actions by transferring their phenolic hydrogen atom to lipid radicals, thus quenching lipid radicals and preventing peroxidation. Since mammalian cells do not synthesize this chain-breaking antioxidant, once membrane vitamin E is consumed as a result of oxidative stress, cellular lipids are highly susceptible to peroxidation that can result in cell death. The generation of reactive oxygen species is believed to play an important role in the pathogenesis of many mitochondrial diseases such as Friedreich's ataxia (FRDA) (9,12). Consistent with this hypothesis, vitamin E deficiency produces a disease very similar to FRDA (20).

α-Tocopherol and its derivatives have been tested clinically for the therapy of diseases associated with oxygen radical production. Recently, it has been demonstrated that the oxidative stability of electron-rich phenolic compounds can be greatly improved by incorporating nitrogen in the aromatic ring (21–23). In a recent study, we have shown that a lipophilic pyridinol analogue of tocopherol was capable of quenching lipid peroxidation more effectively than tocopherol and conferring protection to cultured CEM leukemia cells that had been placed under oxidative stress (24).

The prodrug approach represents a well-known tool widely employed to modify the stability and physicochemical characteristics of active compounds and, consequently, to increase their pharmacological activity and overcome pharmacokinetic limitations. The concept of a prodrug was introduced by Albert in the late 1950s (25), and it is defined as pharmacologically inactive chemical derivative of a parent drug molecule requiring chemical or enzymatic transformation within the body to release the parent drug. Vitamin E is generally administered as a prodrug in the form of tocopheryl acetate to increase stability and solubility of the parent tocopherol. This derivative carries an acetyl moiety at the C-6 phenolic group (Fig. 1) that blocks the antioxidant properties. However, nonspecific esterases cleave the ester bond *in vivo* and release α-tocopherol in its active form.

In the present study, we explored an approach to stabilize compound 1 as a prodrug by acetylation of its phenol moiety. The evaluation of this compound as a potential prodrug is the focus of this study. We investigated and compared directly the antioxidant properties of α-TOH acetate and the acetate of compound 1. Both prodrugs were shown to be activated as a function of time, presumably due to susceptibility to enzymatic hydrolysis, and to exhibit time-dependent increases in antioxidant activity. Diethyl maleate (DEM) and buthionine sulfoximine (BSO) were used to deplete GSH in CEM human leukemia and FRDA fibroblast cells, respectively. Redox-dependent cell death was prevented by inhibition of ROS production, lipid peroxidation and loss of mitochondrial membrane potential ($\Delta\psi_m$) in glutathione-depleted cells pretreated with the acetate of compound 1 or α-tocopherol acetate. We have examined the oxygen free radical scavenging activity of the acetate derivatives of compound 1 and tocopherol in a cell-free system. As expected, neither

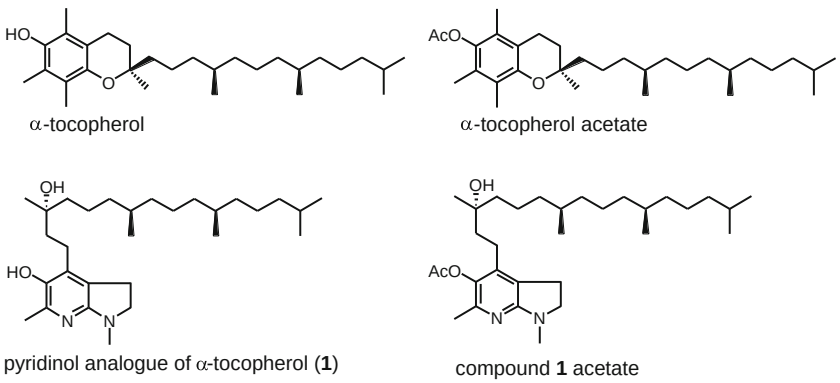

Fig. 1 Chemical structures of vitamin E analogues α-tocopherol (α-TOH), α-tocopherol acetate (α-TOH acetate), pyridinol analogue of α-tocopherol (1), and the *O*-acetate of compound 1.

of the prodrugs exhibited any activity. Acetylation of compound 1 increases its stability and confers properties characteristic of a prodrug, providing a compound that is more effective than α-tocopherol acetate with regard to all protective properties studied.

MATERIALS AND METHODS

Chemicals, including diethyl maleate (DEM), 2,2'-azobis-(2-amidinopropane) dihydrochloride (AAPH), L-buthionine-(*S*, *R*)-sulfoximine (BSO), (+)-alpha-tocopherol (α-TOH), (+)-alpha-tocopherol acetate, trolox, carbonyl cyanide *p*-trifluoromethoxyphenylhydrazone (FCCP) and *N*-acetylcysteine, were purchased from Sigma Aldrich (St. Louis, MO, USA). 1-Stearoyl-2-oleoyl-phosphatidylcholine (SOPC) and 1, 2-dilinoleoylphosphatidylcholine (DLPC) were purchased from Avanti Polar Lipids (Alabaster, AL, USA). Fluorescent probes, including C_{11}-BODIPY$^{581/591}$ (4,4-difluoro-5-(4-phenyl-1,3-butadienyl)-4-bora-3a, 4a-diaza-s-indacene-3-propionic acid), calcein acetoxymethyl (AM), tetramethylrhodamine methyl ester (TMRM), and dichlorodihydrofluorescein diacetate (DCFH-DA), were obtained from Molecular Probes (Eugene, OR, USA). compound 1 and its acetate were prepared as described (24). CEM leukemia cells (ATCC, catalogue number CRL-2264) were cultured in RPMI-1640 medium (Gibco, Grand Island, NY, USA) with 10% fetal calf serum, 2 mM glutamine (HyClone, South Logan, UT, USA) and 1% penicillin–streptomycin antibiotic supplement (Cellgro, Manassas, VA, USA). Cells were passaged daily to maintain them in log phase growth and kept at a nominal concentration of $5–10\times10^5$/mL. Primary fibroblasts were derived from a patient donor with a molecular diagnosis of FRDA. This cell line was obtained from Coriell Cell Repositories (Camden, NJ, USA; catalog number GM-04078). Fibroblasts were cultured in 64% (v/v) Eagle's minimal essential medium (MEM), lacking phenol red with Eagle's balanced salt (EBS) and 25% M199 with EBS (Gibco) supplemented with 15% (v/v) fetal bovine serum albumin (HyClone), 1% penicillin–streptomycin antibiotic mix (Cellgro), 10 μg/mL insulin (Sigma Aldrich), 10 ng/mL basic fibroblast growth factor (βFGF) (Lonza, Walkersville, MD, USA) and 2 mM glutamine. Cells were grown in 75 cm^2 culture flasks and incubated at 37°C in a humidified atmosphere of 5% CO_2 in air. Cells were fed twice weekly and split every third day at a ratio of 1:3.

Assessment of Reactive Oxygen Species Production

Intracellular ROS levels were monitored using 2',7'-dichlorodihydrofluorescein diacetate (DCFH-DA) (26), a membrane-permeable and oxidant-sensitive fluorescent dye. DCFH-DA is a non-fluorescent derivative of fluorescein that emits fluorescence after being oxidized by ROS. DCFH-DA is readily taken up by cells and intracellularly cleaved by endogenous esterases and is retained by viable cells. In the presence of ROS, including hydrogen peroxide, DCFH is oxidized to the highly fluorescent dichlorofluorescein (DCF). Intracellular DCF fluorescence is used as an index of cellular ROS production.

Cellular oxidative stress was induced by pharmacological depletion of glutathione (GSH) using diethyl maleate (DEM) (27–29). ROS production was assessed by monitoring DCF fluorescence. CEM leukemia cells were cultured in RPMI medium with 10% FBS, 2 mM glutamine and 1% penicillin–streptomycin. CEM cells (5×10^5 cell/mL) were plated (1 mL in 12-well plates) and treated with the test compounds at final concentrations of 1 and 5 μM and incubated at 37°C for 1–24 h in a humidified atmosphere containing 5% CO_2 in air. The test compounds were prepared by first making 5 mM stock solutions in DMSO. Cells were treated with 5 mM DEM for 30 min, collected by centrifugation at 300 × g for 3 min, and then washed twice with phosphate-buffered saline. Cells were resuspended in Hanks' balanced salt solution buffer (HSSB) and incubated at 37°C in the dark for 20 min with 10 μM DCFH-DA. Cells were collected by centrifugation at 300 × g for 3 min, then washed twice with phosphate-buffered saline. The samples were analyzed immediately by flow cytometry (Becton-Dickinson FACS Caliber instrument equipped with Cell Quest software, BD Biosciences, Rockville, MD, USA) using a 488 nm excitation laser and FL1-H channel 538 nm emission filter. In each analysis, 10,000 events were recorded. Results obtained were verified by repeating the experiments in triplicate.

Assessment of Lipid Peroxidation

Membranous lipid peroxidation was detected by fluorescence of C_{11}-BODIPY$^{581/59}$, a lipophilic probe incorporated in cellular membranes, where it changes its emitted fluorescence from red to green upon oxidation by lipid radicals (30,31). As the oxidation of C_{11}-BODIPY$^{581/59}$ is proportional to the extent of lipid peroxidation of polyunsaturated fatty acids in the membrane, it can serve as an indicator of lipid peroxidation in cell membranes and membrane model liposomes.

Preparation of Liposomes Vesicles

Phosphatidylcholine liposomes were prepared as described (32). Briefly, 25 mg of DLPC and 25 mg of SOPC were dissolved in chloroform, and the solvent was concentrated to dryness under a stream of nitrogen to give a thin film of phosphatidylcholine in a round-bottomed flask. The lipid film was hydrated with 50 mL of 10 mM Tris–HCl, pH

7.4, containing 100 mM KCl, then shaken and sonicated on ice for 15 s. The liposomes so obtained were filtered through a 0.2 μM membrane filter.

Measurement of C_{11}-BODIPY$^{581/591}$ Oxidation in Membrane Model Liposome Vesicles

C_{11} BODIPY$^{581/591}$ was incorporated into liposomes and oxidized by peroxyl radicals derived from the decomposition of AAPH in presence and absence of the test compounds. Briefly, liposomes (1 mg/mL), suspended in 10 mM Tris–HCl, pH 7.4, containing 100 mM KCl, were transferred to a 1-mL quartz cuvette and placed in a Varian Cary Eclipse fluorometer (Varian, Cary, NC, USA) equipped with a thermostatted cuvette holder at 40°C. Liposomes were pre-incubated at 40°C for 10 min with 200 nM C_{11} BODIPY$^{581/591}$ to allow their incorporation into the lipid phase of the liposomes. After the addition of 10 mM AAPH, the decay of red fluorescence emission was followed at λ_{ex} 570 nm, λ_{em} 600 nm. Relative fluorescence units were normalized to 100% intensity. The results obtained were verified in three independent experiments.

Flow Cytometric Measurement of C_{11}-BODIPY$^{581/591}$ Oxidation in Cell Culture

Lipid peroxidation in CEM leukemia cells was detected by utilizing the oxidant-sensitive lipophilic probe C_{11}-BODIPY$^{581/591}$ as described previously (30,31). Briefly, CEM cells (5×10^5 cell/mL) were treated with the test compounds at final concentrations of 1 and 5 μM and incubated at 37°C for 1–24 h in a humidified atmosphere containing 5% CO_2 in air. Cells were treated with 500 nM C_{11} BODIPY$^{581/591}$ in phenol red-free RPMI-1640 media and incubated at 37°C in the dark for 30 min. Oxidative stress was induced with 5 mM DEM in phenol red-free RPMI-1640 media for 90 min. Treated cells were collected by centrifugation at 300 × g for 3 min and then washed twice with phosphate-buffered saline. Cells were resuspended in 250 μL of phosphate-buffered saline and were analyzed by FACS (FACS Calibur flow cytometer, Becton Dickinson) to monitor the change in intensity of the C_{11} BODIPY$^{581/591}$-green (oxidized) fluorescence signal.

Fluorescent Microscopic Examination of Lipid Peroxidation

Measurement of the extent of lipid peroxidation in FRDA fibroblasts was carried out after treatment with 1 mM BSO, in presence and absence of 5 μM compound 1 acetate or α-tocopherol acetate. Briefly, FRDA fibroblasts (2×10^5 cells/mL) were seeded in cover slips (Corning, Corning, NY, USA) in 6-well plates. The plates were incubated at 37°C overnight in a humidified atmosphere of 5% CO_2 in air to allow attachment of the cells to the cover slips. The following day, cells were treated with 5 μM compound 1 acetate or α-tocopherol acetate and incubated for an additional 12 h before treatment with 1 mM BSO. Lipid peroxidation was assessed after 16 h. The cell culture medium was discarded by aspiration, and each well of the cell culture plate was washed with pre-warmed (37°C) phosphate-buffered saline. The cells were then treated with 1 μM C_{11} BODIPY$^{581/591}$ at 37°C for 30 min. Glass cover slips were rinsed with phosphate-buffered saline and mounted onto slides, and images were recorded and analyzed with a Zeiss AxioCam MRm and AxioVision 3.1 software (Carl Zeiss Goettingen, Germany) on a Zeiss Axiovert 200 M inverted microscope, equipped with a 40x oil immersion objective.

Measurement of Mitochondrial Membrane Potential ($\Delta\psi_m$)

The mitochondrial membrane potential ($\Delta\psi_m$) is a major indicator of mitochondrial function. Higher mitochondrial membrane potential normally implies better mitochondrial function (33). The mitochondrial membrane potential was assessed by TMRM staining. This indicator dye is a lipophilic cation which accumulates within mitochondria in accordance with the $\Delta\psi_m$ Nernst potential (34). Upon accumulation, this dye exhibits a red shift in both absorption and fluorescence emission spectra. The fluorescence intensity is quenched when the dye is accumulated by mitochondria. Briefly, CEM leukemia cells were pre-treated with or without the test compounds for 1–24 h. The cells were treated with 5 mM DEM for 120 min, collected by centrifugation at 300 × g for 3 min, and then washed twice with phosphate-buffered saline. The cells were resuspended in HSSB buffer and incubated at 37°C in the dark for 15 min with 250 nM TMRM. Cells were collected by centrifugation at 300 × g for 3 min and were then washed twice with phosphate-buffered saline. The samples were analyzed immediately by flow cytometry using 488 nm excitation laser and the FL2-H channel. The results obtained were verified in three independent experiments. The protonophore FCCP (30 μM) was used to dissipate the chemiosmotic proton gradient ($\Delta\mu H^+$) and served as a control for loss of $\Delta\psi_m$. In each analysis, 10,000 events were recorded.

Measurement of the Mitochondrial Permeability Transition (MPT)

The MPT was assayed by measuring calcein fluorescence quenched by cobalt ion in mitochondria, as described previously (35), using the MitoProbe Transition Pore Assay

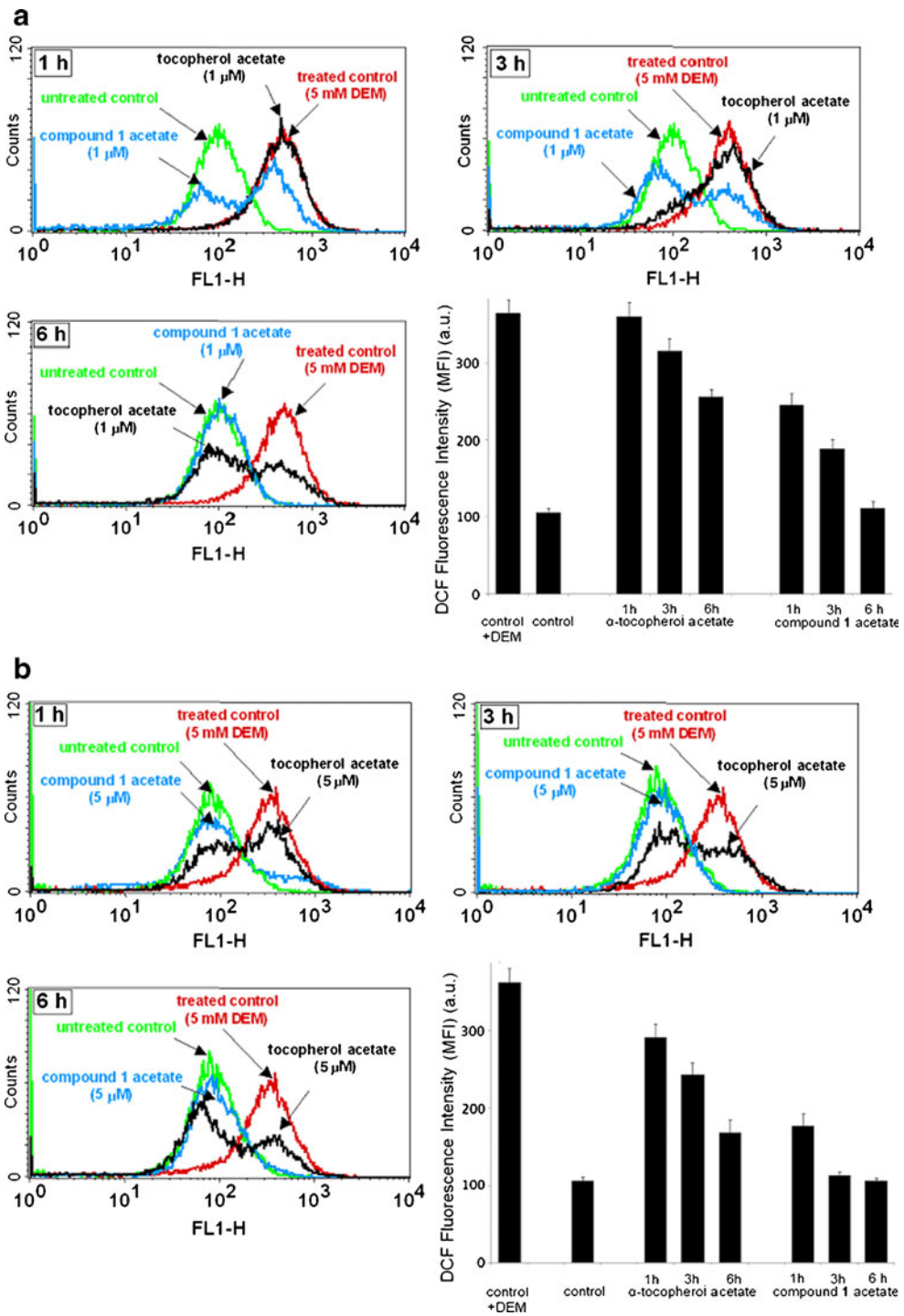

Fig. 2 Representative flow cytometric histograms overlay showing the time-dependent dose response effect of α-TOH and compound 1 acetate on ROS production in glutathione-depleted CEM cells. Following pretreatment with the indicated compounds (1 μM) (**a**) or (5 μM) (**b**) for different time points (1, 3, or 6 h), the cells were treated with or without 5 mM diethyl maleate (DEM) for 30 min to induce oxidative stress by glutathione depletion. The cells were washed twice in phosphate-buffered saline and then suspended in Hanks' Balanced Salt Solution buffer (HSSB). Cells were loaded with 10 μM dichlorodihydrofluorescein diacetate (DCFH-DA) for 20 min in the dark, and the green fluorescence (DCF) was measured by flow cytometry using the FL1-H channel. The figure shows a representative example of three independent experiments. In each analysis, 10,000 events were recorded. Increased DCF fluorescence, a measure of intracellular oxidation and ROS production, was determined by a shift in DCF fluorescence to the right on the *x*-axis of the FACS histogram. The bottom right panel shows a bar graph of mean DCF fluorescence values (a.u.) recorded by FACS and represents the mean fluorescence intensity (MFI) of the flow histogram profiles calculated using CellQuest software. Data are expressed as means ± SE ($n = 3$). compound 1 acetate exhibited better cytoprotection against ROS than α-tocopherol acetate.

Kit (Molecular Probes, Eugene, OR, USA). This method allows direct visualization of permeability changes in mitochondria *in situ*. Upon addition of calcein acetoxymethyl ester, the dye enters the cells and becomes fluorescent upon de-esterification and oxidation. Co-loading of cells with cobalt chloride quenches the fluorescence in the cell, except in mitochondria, as cobalt cannot cross the mitochondrial membrane. When the MPT pore is activated, the fluorescence from the mitochondrial calcein is also quenched by cobalt, and MPT openings can be detected. Briefly, FRDA fibroblasts (2×10^5 cells/mL) were seeded in cover slips (Corning) in 6-well plates. The plates were incubated at 37°C overnight in a humidified atmosphere of 5% CO_2 in air to allow attachment of the cells to the cover slips. The following day, cells were treated with 15 μM compound 1 acetate or α-tocopherol acetate and incubated for an additional 12 h before treatment with 1 mM BSO. Mitochondrial membrane integrity was assessed after 16 h. The cell culture medium was removed by aspiration, and each well was washed twice with pre-warmed (37°C) Hanks' balanced salt solution (144 mM NaCl, 10 mM Hepes, 2 mM $CaCl_2$, 1 mM $MgCl_2$, 5 mM KCl, and 10 mM glucose, pH 7.4). Cells were incubated at 37°C in fresh HSSB containing 1 μM calcein acetoxymethyl ester and co-stained with 50 nM TMRM and 5 μg/mL Hoechst 33342 in the presence of 1 mM cobalt chloride for 20 min. Following cobalt quenching, cover slips were rinsed with phosphate-buffered saline and mounted onto slides, and images were collected within 30 min, as described above. This method has been validated by the addition of 0.5 mM $CaCl_2$ along with the calcium ionophore ionomycin (5 μM) to cultures in (HSSB) previously loaded with calcein and $CoCl_2$.

Trypan Blue Cell Viability Assay

Cell viability was determined by trypan blue exclusion assay. This technique was used to assess the cytoprotective effects of the tested compounds in cultured cells treated with DEM to induce cell death by GSH depletion. The viability of DEM-treated CEM cells was determined by their ability to exclude the dye trypan blue. Viable cells exclude trypan blue, whereas non-viable cells take up the dye and stain blue. Briefly, CEM cells were grown in RPMI 1640 medium (Gibco) supplemented with 10% fetal calf serum, 2 mM glutamine (HyClone) and 1% penicillin–streptomycin mix (Cellgro). Cells were seeded at a density of 5×10^5 cells/mL and treated with different concentrations of the indicated compounds. Cells were incubated at 37°C in a humidified atmosphere of 5% CO_2 in air for 6 or 24 h. After pre-incubation, the cells were treated with 5 mM DEM. Cell viability was determined by staining cells with 0.4% trypan blue using a hemacytometer. At least 500 cells were counted in each experimental group. At the time of assay, >90% of DEM-treated cells were trypan blue positive, whereas in non-DEM-treated control, cell cultures >95% cells were viable. Cell viability was expressed as the percentage of control. Data are expressed as means±S.E.M. ($n=3$).

Fig. 3 (**a**) Redox-silent tocopherol acetate and compound 1 acetate showed no significant protection against lipid peroxidation induced by peroxyl radicals generated from thermal decomposition of AAPH in phospholipid liposomes in Tris-HCl buffer at 40°C. Parent compound 1 showed significant protection against lipid peroxidation as compared with tocopherol by measuring their ability to preserve the fluorescence of C_{11}-BODIPY$^{581/591}$ in presence of 10 mM AAPH. Relative fluorescence units are normalized to 100% intensity. An independent repeat experiment gave identical results. (**b**) Lipid peroxidation in CEM leukemia cells depleted of glutathione. Representative flow cytometric histograms overlay showing lipid peroxidation in CEM cells. Following pretreatment with the indicated compounds at 1 μM concentration for the indicated preincubation time (upper panels) or at 5 μM concentration (lower panels), cells were treated with 500 nM C_{11}-BODIPY$^{581/591}$ in the dark at 37°C for 30 min before inducing lipid peroxidation with 5 mM diethyl maleate (DEM) for 90 min and then subjected to flow cytometry analysis using FL1-H channel for C_{11}-BODIPY$^{581/591}$—green (oxidized form). The figure shows a representative example of three independent experiments. In each analysis, 10,000 events were recorded. Increased C_{11}-BODIPY$^{581/591}$—green fluorescence, a measure of intracellular lipid peroxidation, was determined by a shift in BODIPY$^{581/591}$—green fluorescence to the right on the *x*-axis of the FACS histogram relative to the untreated control. Bottom right of each panel shows a bar graph of mean C_{11}-BODIPY$^{581/591}$—green (oxidized form) fluorescence (a.u.) recorded by FACS and represents the geometric means of the above flow cytogram profiles calculated using CellQuest software. Data are expressed as means±SE (n=3). Compound 1 acetate showed better protection against lipid peroxidation than α-tocopherol acetate in a concentration- and time-dependent fashion. (**c**) Effect of the two prodrugs, α-tocopherol acetate and compound 1 acetate, on lipid peroxidation in cultured primary fibroblasts from a Friedreich's ataxia patient (GM-04078) after treatment with buthionine sulfoximine (BSO). Fluorescence microscopy analysis of FRDA fibroblasts stained with C_{11}-BODIPY$^{581/591}$ red (reduced form) and co-stained Hoechst 33342. Red fluorescence (C_{11}-BODIPY$^{581/591}$ red (reduced form)) represents non-oxidized lipids, and green fluorescence (C_{11}-BODIPY$^{581/591}$ green (oxidized form)) represents oxidized lipids. Panels i, ii, iii, and iv represent untreated control, treated control (BSO, 16 h), compound 1 acetate (5 μM), and tocopherol acetate (5 μM) respectively.

RESULTS

Compound 1 Acetate Reduces ROS Levels in Glutathione-Depleted CEM Leukemia Cells

GSH is a physiological oxidant scavenger, reacting as either a one-electron donor to radicals or a two-electron donor to electrophiles, and occurs in all mammalian cell types (36). Lowering GSH levels in CEM cells was found to cause a significant increase in both cellular and mitochondrial ROS levels (27,29). Therefore, we analyzed the ROS levels in DEM-treated CEM leukemia cells using DCFH-DA, which is converted to DCF by ROS-mediated oxidation (26). Cells stained with DCF were analyzed by fluorescent-activated

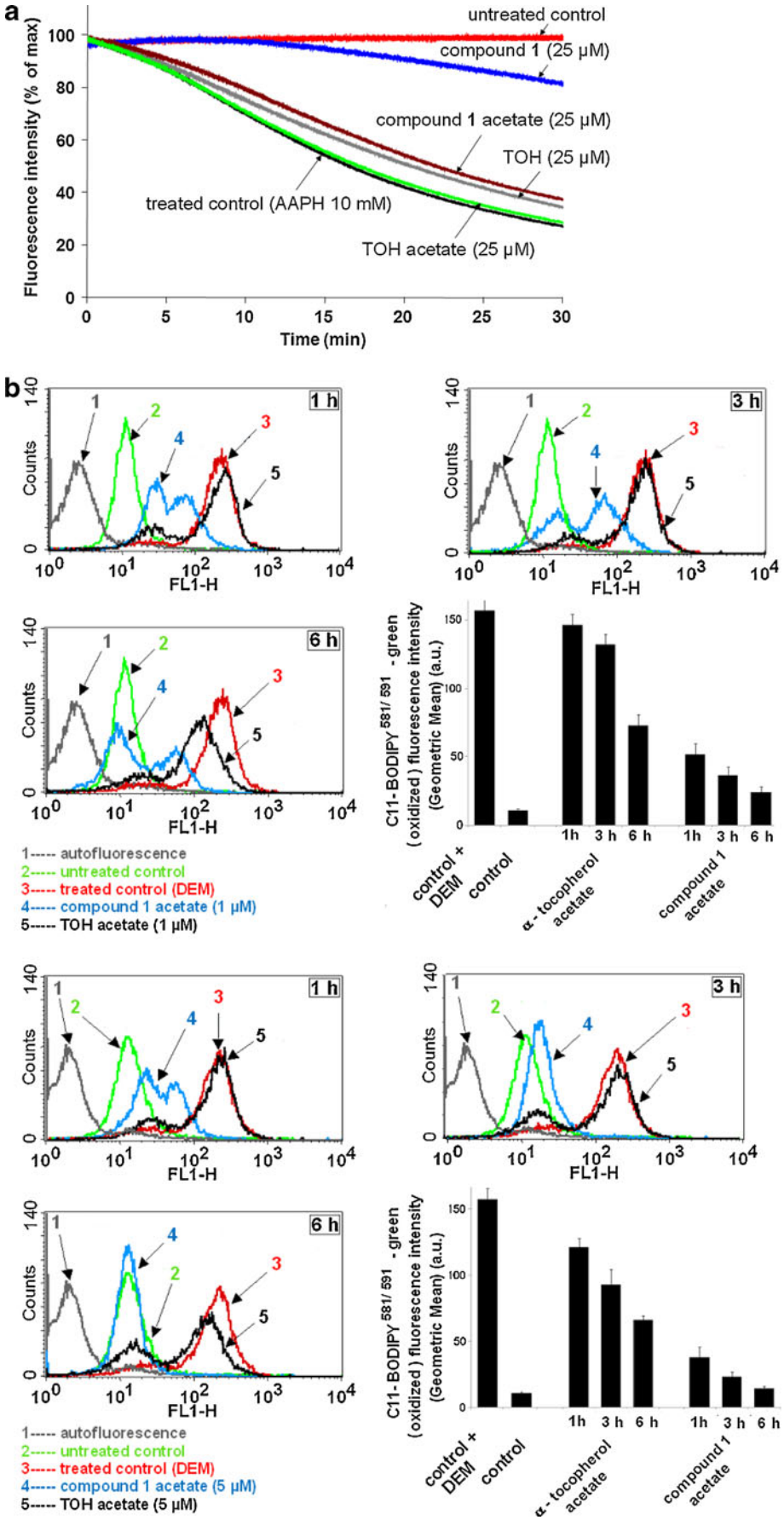
a
untreated control
compound 1 (25 μM)
compound 1 acetate (25 μM)
TOH (25 μM)
treated control (AAPH 10 mM)
TOH acetate (25 μM)
Fluorescence intensity (% of max)
Time (min)
b
1 h
3 h
6 h
Counts
FL1-H
1-----autofluorescence
2-----untreated control
3-----treated control (DEM)
4-----compound 1 acetate (1 μM)
5-----TOH acetate (1 μM)
C11-BODIPY 581/591 - green (oxidized) fluorescence intensity (Geometric Mean) (a.u.)
control + DEM
control
α - tocopherol acetate
compound 1 acetate
1h 3 h 6 h 1h 3 h 6 h
1-----autofluorescence
2-----untreated control
3-----treated control (DEM)
4-----compound 1 acetate (5 μM)
5-----TOH acetate (5 μM)

Fig. 3 (continued)

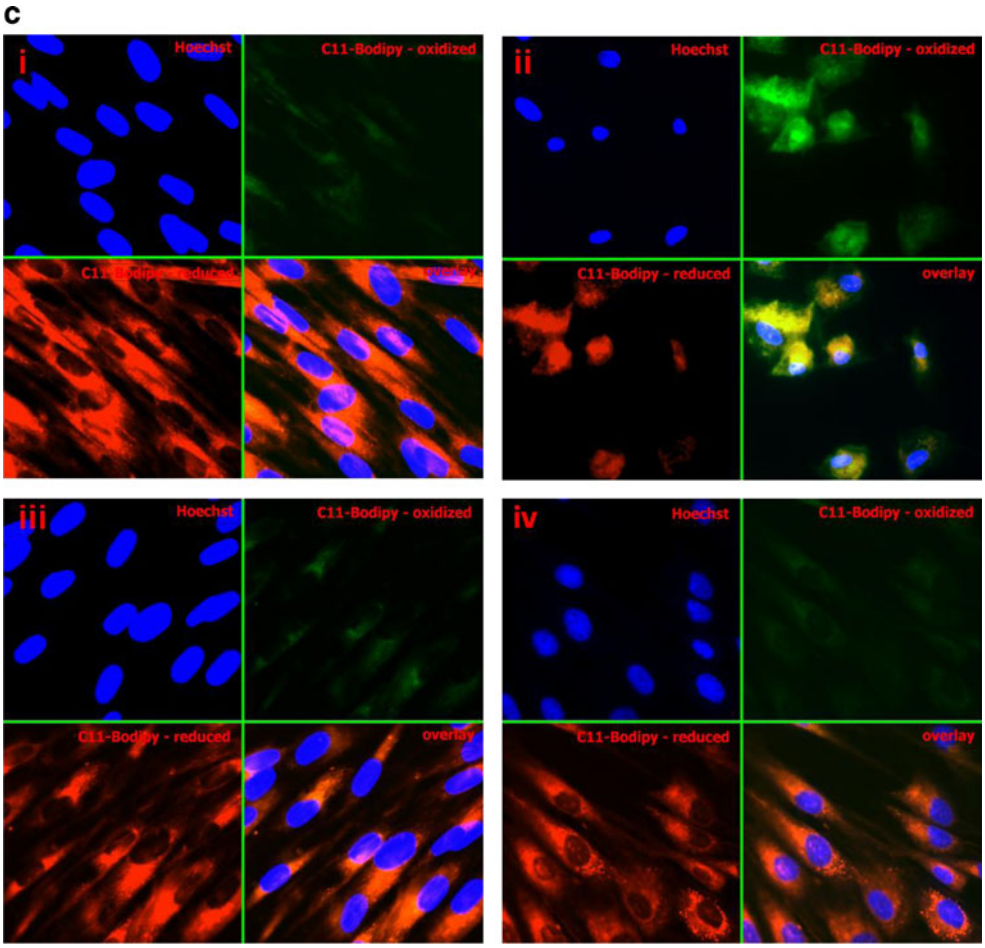

cell sorting. Figure 2 shows representative DCF overlay FACS histograms of CEM cells stained with DCFH-DA and analyzed, as described in "Materials and Methods." The results clearly show a significant decrease in the intensity of DCF fluorescence in a concentration- and time-dependent manner. Pre-incubation with 1 μM compound 1 acetate resulted in complete protection against ROS after 6 h, while the use of 5 μM compound 1 acetate afforded protection after 3-h preincubation. α-TOH acetate was fully protective only after 12 h preincubation (see Supplemental Material Figure S1).

Assessment of Lipid Peroxidation in a Cell-Free Membrane Model System

The ability of α–tocopherol acetate and compound 1 acetate to quench lipid peroxidation using a C_{11}-BODIPY$^{581/591}$ liposome system initiated by addition of the free radical generator 2,2'-azobis-(2-amidinopropane) dihydrochloride (AAPH) was assessed as illustrated in Fig. 3a. Formation of lipid peroxides was quantified using the fluorescent lipophilic probe C_{11}-BODIPY$^{581/591}$, which relies on the trapping of peroxyl radicals. The use of liposomes incorporating C_{11}-BODIPY$^{581/591}$, with peroxynitrite, resulted in apparent peroxidation, since oxidation of this probe results in a change of its emitted fluorescence from red to green (30,31). The parent compound (compound 1) was more effective in preventing lipid peroxidation than α-TOH (Fig. 3a). As anticipated, neither of the acetate derivatives (prodrugs) had any significant effect on quenching lipid peroxidation in the cell-free system.

Assessment of Lipid Peroxidation in Cultured Cells

Lipid peroxidation was determined in CEM leukemia cells by monitoring the fluorescence of the peroxidation-sensitive dye C_{11}-BODIPY$^{581/591}$, which incorporates into membranes. Increased C_{11}-BODIPY$^{581/591}$-green (oxidized) fluorescence, a measure of peroxyl radical production, was determined by a shift in green fluorescence to the right on the *x*-axis of the FACS histogram. Figure 3b shows representative BODIPY$^{581/591}$-green FACS histograms overlay of CEM leukemia cells stained with BODIPY$^{581/591}$-red (reduced) and analyzed using the FL1-H channel, as described in "Materials and Methods." Glutathione depletion by DEM treatment caused the BODIPY$^{581/591}$-green fluorescence to shift right

on the *x*-axis of the FACS histogram (Fig. 3b), indicating increased peroxidation as a result of glutathione depletion. Pretreatment of the CEM cells with compound 1 acetate blocked lipid peroxidation in both a concentration- and time-dependent manner. α-TOH acetate showed partial or no protection at preincubation times up to 6 h, but was essentially equally as effective as compound 1 acetate after 24 h (Fig. 3b and Supplementary Material Fig. S2).

Similar results were obtained using fluorescence microscopy analysis in cultured primary fibroblasts from a Friedreich's ataxia patient (GM-04078) after glutathione depletion resulting from buthionine sulfoximine (BSO) treatment for 16 h. Fluorescent microscopy analysis revealed that FRDA fibroblasts treated with 1 mM BSO were significantly under oxidative stress, as shown by increasing in $BODIPY^{581/591}$-green (oxidized) (Fig. 3c). Fig. 3c shows that oxidation of $BODIPY^{581/59}$ is strongly attenuated when Friedreich's fibroblasts were pretreated with α-TOH acetate or compound 1 acetate at 5 μM concentration.

Compound 1 Acetate Protects Against DEM-Induced Mitochondrial Membrane Depolarization in Cultured CEM Leukemia Cells

To demonstrate that reduction in mitochondrial oxidative stress can protect against mitochondrial dysfunction, we examined the effect of the pyridinol-based tocopherol acetate analogue on mitochondrial membrane depolarization caused by treatment of CEM leukemia cells with DEM. Mitochondrial membrane depolarization is a critical antecedent event to cell death. TMRM, a fluorescence cationic indicator, is taken up into mitochondria in a potential-dependent manner, and the opening of the mitochondrial permeability transition pore and depolarization leads to diminished labeling of the mitochondria by the fluoroprobe. We used Mitotracker TMRM to determine whether compound 1 acetate preserves mitochondrial membrane polarization. Figure 4 illustrates representative two-dimensional density dot plots of TMRM-stained cells showing the percentage of cells with intact $\Delta\psi_m$ (TMRM fluorescence in top right quadrant) *vs* the percentage of cells with reduced $\Delta\psi_m$ (TMRM fluorescence in bottom left and right quadrants). Figure 4a,b (bottom panels) shows bar graphs of the percentage (mean±S.E.) of CEM cells with intact $\Delta\psi_m$. The results show that DEM treatment reduced the percentage of cells with TMRM fluorescence in the top right quadrant, indicating that DEM treatment caused depolarization of $\Delta\psi_m$. Once again, $\Delta\psi_m$ protection was both concentration- and time-dependent (Fig. 4, Supplementary Material Fig. S3). As illustrated in Fig. 4a, preincubation the CEM cells for 6 h with 1 μM test compounds prior to stressing the cells with DEM resulted in nearly full protection by compound 1 acetate, but only partial (50%) protection by tocopherol acetate (top panel a). Increasing the concentration of test compounds to 2.5 μM resulted in increasing protection (top panel b). The ability of the parent compound 1 to protect the mitochondrial membrane diminished as the preincubation time was increased to 24 h (Supplementary Material Fig. S3).

Compound 1 Acetate Protects Against DEM-Induced Mitochondrial Permeability Transition (MPT) in Cultured Primary FRDA Fibroblasts

Oxidative stress, in addition to resulting in mitochondrial calcium overload, is known to trigger the MPT and can be induced by glutathione depletion (37,38). The role of the mitochondrial permeability transition in cell physiology and pathology is still controversial, in part because of lack of an appropriate method for direct demonstration of MPT in intact cells. The MPT is a Ca^{2+}-dependent process often associated with oxidative stress and various other factors (39). As the identity of individual components of the MPT pore remains controversial, the MPT is characterized by opening of the permeability transition pore in the inner mitochondrial membrane that increases permeability and leads to collapse of $\Delta\psi_m$ and cell death.

To determine the changes in mitochondrial permeability and membrane potential, a double-staining method with fluorescent dyes, calcein-AM and tetramethylrhodamine fluorescent methyl ester (TMRM), was used as described before (35) with some modification. TMRM is a cell-permeable, voltage-sensitive dye that accumulates in energized, but not depolarized, mitochondria. As cobalt is impermeable to the inner mitochondrial membrane, it does not enter the mitochondria, so calcein in the mitochondria is not quenched. Under normal conditions, both TMRM and calcein colocalized in the mitochondria as shown in Fig. 5 (a). However, glutathione depletion induces the mitochondrial permeability transition (37,38), making the mitochondria permeable to solutes, and depolarizes the membrane potential. Thus, mitochondria lose TMRM and become permeable to cobalt, which quenches mitochondrial calcein as shown in a redox-dependent MPT in glutathione-depleted cells (Fig. 5b). As shown in Fig. 5c and d, both prodrugs prevented BSO-induced MPT in FRDA fibroblasts.

Compound 1 Acetate Blocks Cell Death in Cultured CEM Leukemia Cells After GSH Depletion

Since α-tocopherol acetate and compound 1 acetate blocked ROS production and lipid peroxidation and preserved mitochondrial structure in cultured cells, it was logical to believe that they might enhance cell viability. Accordingly, we determined cell viability after DEM treatment of the cells. Figure 6 shows that compound 1 acetate was

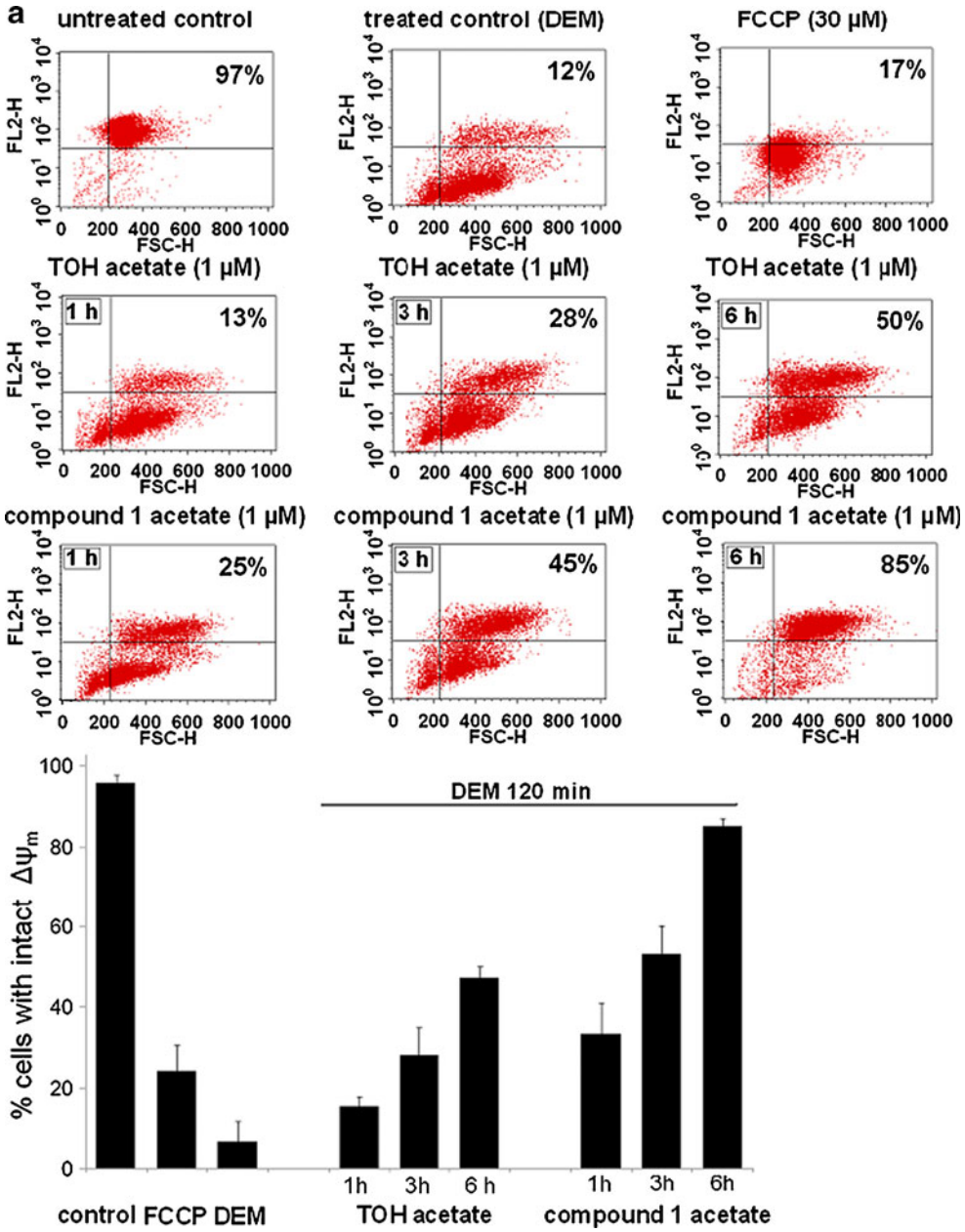

Fig. 4 Representative flow cytometric two-dimensional color density dot plot analyses of mitochondrial membrane potential $\Delta\psi_m$ in CEM cells stained with 250 nM TMRM and analyzed using the FL2-H channel as described in "Materials and Methods." Following pretreatment with the indicated compounds (1 μM or 2.5 μM) for the indicated preincubation time, the cells were treated with 5 mM diethyl maleate (DEM) for 120 min. The cells were washed twice in phosphate-buffered saline and suspended in Hanks' Balanced Salt Solution buffer. Cells were loaded with 250 nM TMRM for 15 min, and the red fluorescence was measured by flow cytometry using the FL2-H channel. The percentage of cells with intact $\Delta\psi_m$ is indicated in the top right quadrant of captions. Representative example from at least three independent experiments. In each analysis, 10,000 events were recorded. Bottom panel shows a bar graph of means the percentage of cells with intact $\Delta\psi_m$ recorded by FACS. Data are expressed as means±SE ($n=3$).

effective in preventing loss of cell viability in CEM cell after treatment with DEM and did so in a concentration-dependent manner. α-Tocopherol acetate was less effective in protecting the CEM cells at all tested concentrations.

DISCUSSION

Beyond a fundamental role in energy metabolism, mitochondria also play key roles in maintenance of cellular redox potential, calcium homeostasis, as well as apoptosis and cell death. In addition, mitochondria are both a major source of reactive oxygen species (ROS) and a target for their damaging effects. In recent years a number of pharmacological antioxidant strategies have been developed aimed at blocking ROS production and lipid peroxidation (15,16). In order to develop novel antioxidants better than vitamin E, several attempts to synthesize vitamin E analogues have been reported (40–45). Recently, we reported a new synthetic analogue of α-tocopherol (compound 1) which was more effective than α-tocopherol as scavenger of reactive oxygen species in glutathione-depleted leukemia CEM cells and prevented lipid peroxidation in mitochondrial membranes (24). To improve stability, vitamin E is commonly used as a non-active esterified prodrug. Such esters are believed to be hydrolyzed *in vivo* by nonspecific esterases to the free active

Fig. 4 (continued)

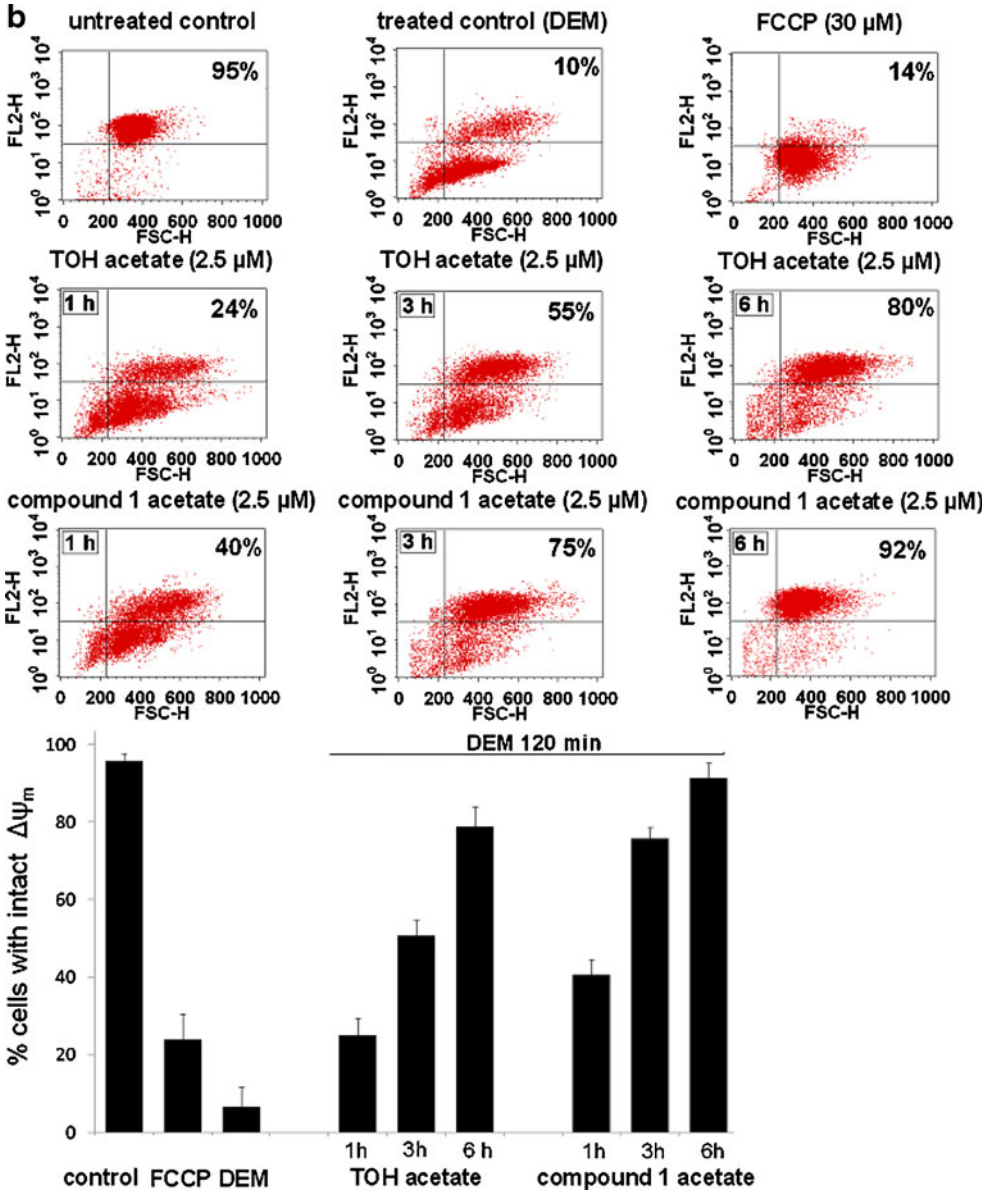

form of the compound. In the present study, we adopted this approach by acetylation of the phenolic OH group of compound 1.

The cytoprotective properties of the derived acetate were characterized using cultured CEM leukemia and FRDA fibroblast cells depleted of glutathione (GSH). Diethyl maleate treatment at 5 mM concentration rapidly depletes cellular glutathione (GSH) and results in lipid peroxidation and necrotic cell death in cultured CEM leukemia cells (27–29). Primary fibroblasts in cell culture lose viability when depleted of GSH using L-buthionine-(*S*,*R*)-sulfoximine (BSO), which irreversibly blocks γ-glutamyl cysteine synthase, the rate-limiting enzyme in glutathione synthesis (46). Fibroblasts from FRDA patients, but not normal cells, die after GSH depletion resulting from treatment with BSO; this effect can be blocked by antioxidants (47). To evaluate compound 1 acetate as a potential prodrug capable of protecting mitochondrial functions, several types of experiments were done.

GSH-depleting agents can induce rapid peroxidation of cellular lipids due to the increased production of ROS (48). In this study, oxidative stress was induced by GSH depletion, and compound 1 acetate potently inhibited the increase in ROS in a concentration- and time-dependent manner. The timing of treatment (1–24 h) of CEM cells with the tested compounds prior to stressing the cells with diethyl maleate can be important, as shown in Fig. 2, and Supplementary Material Fig. S1). Pretreatment of CEM cells with 1 or 5 μM α-tocopherol acetate for short time periods (1–6 h) prior to DEM treatment resulted in incomplete or partial protection,

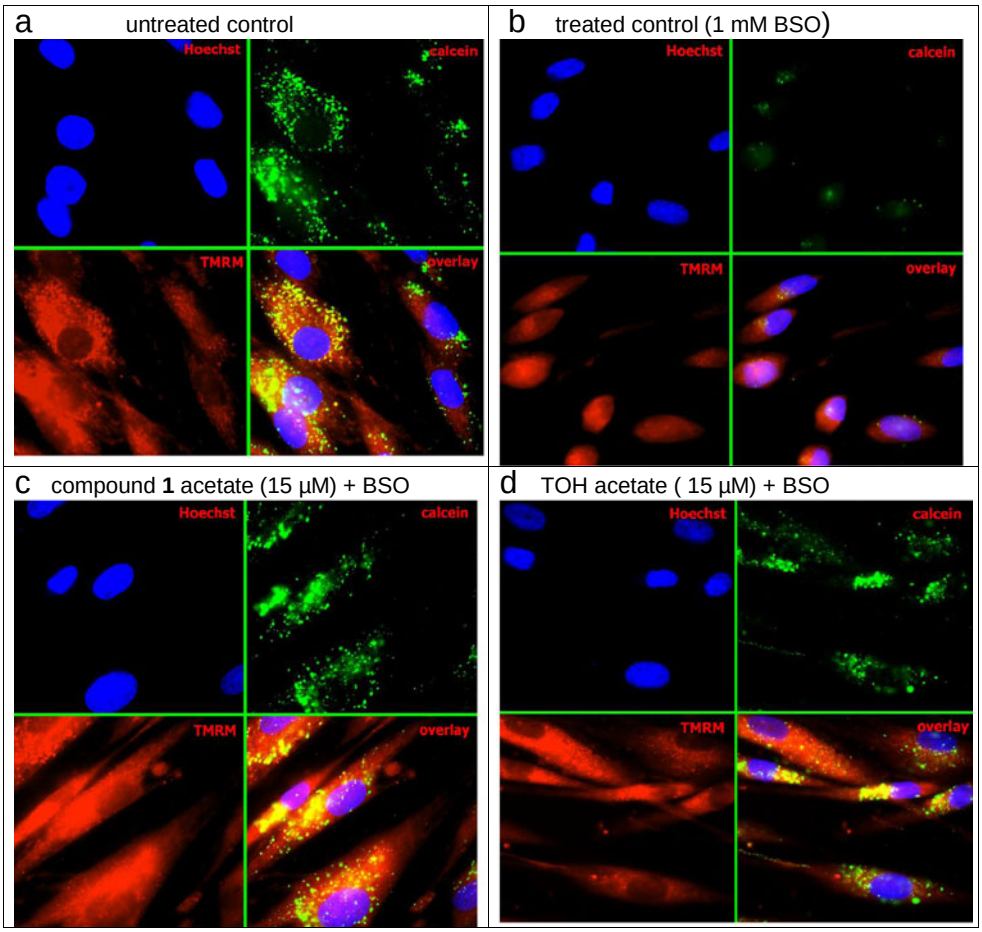

Fig. 5 Effects of the two prodrugs (α-tocopherol acetate and compound 1 acetate) in blocking the induction of the MPT in BSO-stressed cultured primary fibroblasts from a Friedreich's ataxia patient (GM-04078). Calcein-cobalt quenching assay was used for the evaluation of opening of the mitochondrial permeability transition pore. Mitochondria were co-stained with TMRM (50 nM); nuclei were stained with Hoechst 33342 (5 μg/mL). The representative fluorescence microscopy images of calcein signal (green) that were overlapped with TMRM (red) was shown. (**a**–**d**) Untreated control, treated control (BSO, 16 h), compound 1 acetate (15 μM), and tocopherol acetate (15 μM) respectively.

whereas compound 1 acetate afforded complete protection after 6 h at 1 μM concentration and 3 h at 5 μM (Fig. 2). After a 24-h preincubation, both compounds were able to afford complete protection against DEM-induced oxidative stress (Supplementary Material Fig. S1).

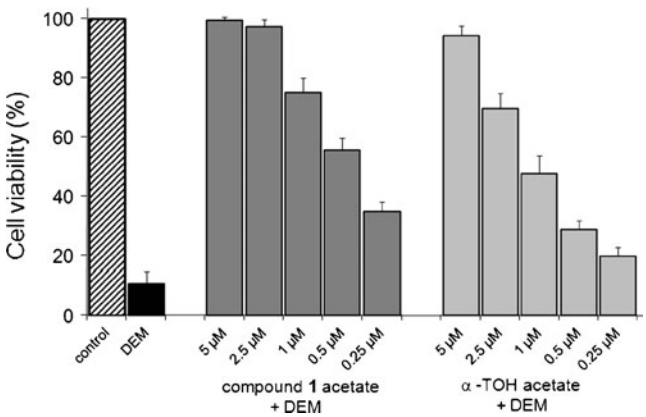

Fig. 6 Trypan blue exclusion assay of CEM cells treated with test compounds. CEM cells were incubated in RPMI medium (control) with compound 1 acetate, or α-tocopherol acetate for 24 h, followed by 5 mM DEM treatment. Cell viability was determined by trypan blue exclusion analysis at 4 h after DEM treatment. At least 500 cells were counted for each experimental group. At the time of assay, >90% of the DEM-treated cells were trypan blue positive; in non-DEM treated control cell cultures >95% cells were viable. Cell viability was expressed as the percentage of control. Data are expressed as means±S.E.M. ($n=3$).

Assessment of oxidative membrane injury has been approached through a variety of biochemical and biophysical methods, and such measurements provide an important analytical index that can be used to evaluate membrane damage (49). In the cell-free system used here, as expected, both compounds lacked any significant effect in quenching lipid peroxidation, whereas parent compound 1 largely prevented lipid peroxidation initiated by the thermal decomposition of AAPH (Fig. 3a). The lack of activity of the acetates is certainly due to the absence of enzymatic transformation of the prodrugs to their active forms. C_{11}-BODIPY$^{581/591}$ was also used as a redox-sensitive lipid peroxidation reporter in living cells; its fluorescence changes irreversibly from red to green upon exposure to ROS (30,31). compound 1 acetate was more effective in blocking lipid peroxidation in DEM-treated CEM cells than was α-tocopherol. Again, the effect was both concentration- and time-dependent (Fig. 3b). α-Tocopherol failed to confer any protection at short preincubation time prior to stressing the cell with DEM. The shift of the fluorescence from red to green correlated well with the formation of phospholipid peroxides. This was determined by a shift in

green fluorescence to the right on the *x*-axis of the FACS histogram (Fig. 3b). Similar results were obtained using C_{11}-BODIPY$^{581/591}$ for fluorescence microscopy analysis of lipid peroxidation in FRDA fibroblasts treated with BSO. FRDA cell monolayers were stained with the fluorescent probe (Fig. 3c). The dye is incorporated into the phospholipid membrane due to its hydrophobicity. Those cells untreated with any oxidant were bright red (Fig. 3c, i), suggesting a normal state, while cells treated with BSO were bright green due to oxidation of the phenyldiene side chain by peroxyl radicals (Fig. 3c, ii). In Fig. 3, iii and iv, it is shown that oxidation of C_{11}-BODIPY$^{581/591}$ was strongly attenuated when FRDA fibroblasts were pretreated with α-tocopherol acetate and compound 1 acetate.

Compound 1 acetate effectively prevented the loss of $\Delta\psi_m$ in a concentration- and time-dependent manner (Fig. 4). Once again, α-tocopherol acetate was not effective in maintaining $\Delta\psi_m$ at shorter preincubation times prior to stressing the cells with DEM (Fig. 4). After a 24-h preincubation, both compounds afforded complete protection against loss of $\Delta\psi_m$ under DEM-induced oxidative stress (not shown).

We found that compound 1 acetate prevented mitochondrial membrane permeabilization in FRDA cells after BSO treatment (Fig. 5) and the death of cultured CEM cells after GSH depletion (Fig. 6). The mechanisms of protection likely involved scavenging ROS production, quenching lipid peroxidation, and preservation of mitochondrial protein thiol redox status, which prevented the loss of $\Delta\psi_m$ and precluded the mitochondrial permeability transition. The present work establishes the antioxidant properties of this prodrug in inhibiting mitochondrial lipid peroxidation, as well as the occurrence of Ca^{2+} activation of mitochondrial permeability transition pore and depolarization. These observations are consistent with the hypothesis that oxidation of critical thiols or other oxidant-sensitive functionalities underlies the mechanisms for the induction of Ca^{2+}-induced MPT and mitochondrial dysfunction (50).

ACKNOWLEDGMENTS & DISCLOSURES

This work was supported in part by a research grant from the Friedreich's Ataxia Research Alliance.

REFERENCES

1. McBride HM, Neuspiel M, Wasiak S. Mitochondria: more than just a powerhouse. Curr Biol. 2006;16:R551–60.
2. Graier WF, Frieden M, Malli R. Mitochondria and Ca^{2+} signaling: old guest, new functions. Eur J Phys. 2007;455:375–96.
3. Bras M, Queenan B, Susin SA. Programmed cell death *via* mitochondria different modes of dying. Biochemistry (Moscow). 2005;70:231–9.
4. Murphy MP. How mitochondria produce reactive oxygen species. Biochem J. 2009;417:1–13.
5. Turrens JF. Mitochondrial formation of reactive oxygen species. J Physiol. 2003;552:335–44.
6. Fridovich I. Fundamental aspect of reactive oxygen species, or what's the matter with oxygen? Ann N Y Acad Sci. 1999;893:13–8.
7. Mates JM, Perez-Gomez C, Nunez de Castro I. Antioxidant enzymes and human diseases. Clin Biochem. 1999;32:595–603.
8. Gaetani GF, Galiano S, Canepa L, Ferraris AM, Kirkman H. Catalase and glutathione peroxidase are equally active in detoxification of hydrogen peroxide in human erythrocytes. Blood. 1989;73:334–9.
9. Armstrong JS, Khdour OM, Hecht SM. Does oxidative stress contribute to the pathology of Friedreich's Ataxia? A radical question. FASEB J. 2010;24:2152–63.
10. Markesbery WR, Carney JM. Oxidative stress in Alzheimer's disease. Brain Pathol. 1999;9:133–46.
11. Barnham KJ, Masters CL, Bush AI. Neurodegenerative diseases and oxidative stress. Nat Rev Drug Discov. 2004;3:205–14.
12. Calabrese V, Lodi R, Tonon C, D'Agata V, Sapienza M, Scapagnini G, *et al.* Oxidative stress, mitochondrial dysfunction and cellular stress response in Friedreich's ataxia. J Neurol Sci. 2005;233:145–62.
13. Lin MT, Beal MF. Mitochondrial dysfunction and oxidative stress in neurodegenerative diseases. Nature. 2006;443:787–95.
14. DiMauro S, Schon EA. Mitochondrial disorders in the nervous system. Annu Rev Neurosci. 2008;31:91–123.
15. Parikh S, Saneto R, Falk MJ, Anselm I, Cohen BH, Hass R. A modern approach to the treatment of mitochondrial disease. Curr Treatm Opt Neurol. 2009;11:414–30.
16. Taylor RW, Chinnery PF, Clark KM, Lightowlers RN, Turnbull DM. Treatment of mitochondrial disease. J Bioenerg Biomembr. 1997;29:195–205.
17. Tucker JM, Townsend DM. Alpha-tocopherol: roles in prevention and therapy of human disease. Biomed Pharmacother. 2005;59:380–7.
18. Lucarini M, Pedulli GF. Bond dissociation enthalpy of α–tocopherol and other phenolic antioxidants. J Org Chem. 1994;59:5063–70.
19. Burton GW, Ingold KU. Vitamin E: application of the principles of physical organic chemistry to the exploration of its structure and function. Acc Chem Res. 1986;19:194–201.
20. Ouahchi K, Arita M, Kayden H, Hentati F, Ben Hamida M, Sokol R, *et al.* Ataxia with isolated vitamin E deficiency is caused by mutations in the alpha-tocopherol transfer protein. Nat Genet. 1995;9:141–5.
21. Prat DA, DiLabio GA, Brigati G, Pedulli GF, Valgimigli LJ. 5-Pyrimidinols: Novel chain-breaking antioxidants more effective than phenols. J Am Chem Soc. 2001;123:4625–6.
22. Wijtmans M, Pratt DA, Brinkhorst J, Serwa R, Valgimigli L, Pedulli GF, *et al.* Synthesis and reactivity of some 6-substituted-2,4-dimethyl-3-pyridinols, a novel class of chain-breaking antioxidants. J Org Chem. 2004;69:9215–23.
23. Wijtmans M, Pratt DA, Valgimigli L, DiLabio GA, Pedulli GF, Porter NA. 6-Amino-3-pyridinols: towards diffusion-controlled chain-breaking antioxidants. Angew Chem Int Ed. 2003;42:4370–3.
24. Lu J, Khdour OM, Armstrong JS, Hecht SM. Design, synthesis and evaluation of an α-tocopherol analogue as a mitochondrial antioxidant. Bioorg Med Chem. 2010;18:7628–38.
25. Albert A. Chemical aspects of selective toxicity. Nature. 1958;182:421–3.

26. LeBel CP, Ishiropoulos H, Bondy SC. Evaluation of the probe 2′,7′- dichlorofluorescein as an indicator of reactive oxygen species formation and oxidative stress. Chem Res Toxicol. 1992;5:227–31.
27. Chua YL, Zhang D, Boelsterli U, Moore PK, Whiteman M, Armstrong JS. Oltipraz-induced phase 2 enzyme response conserved in cells lacking mitochondrial DNA. Biochem Biophys Res Commun. 2005;337:375–81.
28. Zhang D, Lu C, Whiteman M, Chance B, Armstrong JS. The mitochondrial permeability transition regulates cytochrome c release for apoptosis during endoplasmic reticulum stress by remodeling the cristae junction. J Biol Chem. 2008;283:3476–86.
29. Lu C, Armstrong JS. Role of calcium and cyclophilin D in the regulation of mitochondrial permeabilization induced by glutathione depletion. Biochem Biophys Res Commun. 2007;363:572–7.
30. Pap EHW, Drumman GPC, Winter VJ, Kooij TWA, Rijken P, Wirtz KWA, *et al.* Ratio-fluorescence microscopy of lipid peroxidation in living cells using C11-BODIPY$^{581/591}$. FEBS Lett. 1999;453:278–82.
31. Drummen GP, van Liebergen LC, Op den Kamp JA, Post JA. C11-BODIPY (581/591), an oxidation-sensitive fluorescent lipid peroxidation probe: (micro) spectroscopic characterization and validation of methodology. Free Radic Biol Med. 2002;33:473–90.
32. Wu GS, Stein RA, Mead FJ. Autoxidation of phosphatidylcholine liposomes. Lipids. 1982;17:403–13.
33. Bernardi P, Krauskopf A, Basso E, Petronilli V, Blachly-Dyson E, Di Lisa F, *et al.* The mitochondrial permeability transition from *in vitro* artifact to disease target. FEBS J. 2006;273:2077–99.
34. Ehrenberg B, Montana V, Wei M-D, Wuskell JP, Loew LM. Membrane potential can be determined in individual cells from the Nernstian distribution of cationic dyes. Biophys J. 1988;53:785–94.
35. Petronilli V, Miotto G, Canton M, Brini M, Colonna R, Bernardi P, *et al.* Transient and long-lasting openings of the mitochondrial permeability transition pore can be monitored directly in intact cells by changes in mitochondrial calcein fluorescence. Biophys J. 1999;765:725–54.
36. Dalton TP, Chen Y, Schneider SN, Nebert DW, Shertzer HG. Genetically altered mice to evaluate glutathione homeostasis in health and disease. Free Radic Biol Med. 2004;37:1511–26.
37. Petronilli V, Costantini P, Scorrano L, Colonna R, Passamonti S, Bernardi P. The voltage sensor of the mitochondrial permeability transition pore is tuned by the oxidation-reduction state of vicinal thiols: increase of the gating potential by oxidants and its reversal by reducing agents. J Biol Chem. 1994;269:16638–42.
38. Armstrong JS, Jones DP. Glutathione depletion enforces the mitochondrial permeability transition and causes cell death in Bcl-2 overexpressing HL60 cells. FASEB J. 2002;16:1263–5.
39. Zoratti M, Szabo I. The mitochondrial permeability transition. Biochim Biophys Acta. 1995;1241:139–76.
40. Ingold KU, Burton GW, Foster DO, Zuker M, Hughes L, Lacelle S, *et al.* A new vitamin E analogue more active than α-tocopherol in the rat curative myopathy bioassay. FEBS Lett. 1986;205:117–20.
41. Iuliano L, Pedersen JZ, Camastra C, Bello V, Ceccarelli S, Violi F. Protection of low density lipoprotein oxidation by the antioxidant agent IRFI005, a new synthetic hydrophilic vitamin E analogue. Free Radic Biol Med. 1999;26:858–68.
42. Manfredini S, Vertuani S, Manfredi B, Rossoni G, Calviello G, Palozza P. Novel antioxidant agents deriving from molecular combinations of vitamins C and E analogues: 3,4-dihydroxy-5(R)-[2(R, S)-(6-hydroxy-2,5,7,8-tetramethyl-chroman-2(R, S)-yl-methyl)-[1,3]-dioxolan-4(S)-yl]-5H-furan-2-one and 3-O-octadecyl derivatives. Bioorg Med Chem. 2000;8:2791–801.
43. Nam TG, Rector CL, Kim HY, Sonnen AF, Meyer R, Nau WM, *et al.* Tetrahydro-1,8-naphthyridinol analogues of alpha-tocopherol as antioxidants in lipid membranes and low-density lipoproteins. J Am Chem Soc. 2007;129:10211–9.
44. Palozza P, Simone R, Picci N, Buzzoni L, Ciliberti N, Natangelo A, *et al.* Design, synthesis, and antioxidant potency of novel alpha-tocopherol analogues in isolated membranes and intact cells. Free Radic Biol Med. 2008;44:1452–64.
45. Mahdavian E, Sangsura S, Landry G, Eytina J, Salvotore BA. A novel synthesis of tocopheryl amines and amide. Tetrahedon Lett. 2009;50:19–21.
46. Griffith OW, Meister A. Potent and specific inhibition of glutathione synthesis by buthionine sulfoximine (*S*-n-butyl homocysteine sulfoximine). J Biol Chem. 1979;254:7558–60.
47. Jauslin ML, Wirth T, Meier T, Schoumacher F. A cellular model for Friedreich Ataxia reveals small-molecule glutathione peroxidase mimetics as novel treatment strategy. Hum Mol Genet. 2002;11:3055–63.
48. Tirmenstein MA, Nicholls-Grzemski FA, Zhang JG, Fariss MW. Glutathione depletion and the production of reactive oxygen species in isolated hepatocyte suspensions. Chem Biol Interact. 2000;127:201–17.
49. Van Ginkel G, Sevanian A. Lipid peroxidation-induced membrane structural alteration. Methods Enzymol. 1994;233:273–80.
50. Kanno T, Sato EF, Utsumi T, Yoshioka T, Inone M, Utsumi K. Oxidative stress underlies the mechanism for Ca^{2+} -induced permeability transition of mitochondria. Free Radic Res. 2004;38:27–35.